ORIGINAL RESEARCH

Enhancement of the Electro-Optical, Photoluminescent and Plasmonic properties of Gold Nano Particles (GNPs) doped Cholesteric Liquid Crystals Matrix

Article history:
Received: 08-03-2024
Revised: 21-08-2024
Accepted: 05-09-2024
Published: 04-12-2024

Manisha Chaudhary[a], Monika Yadav[b] , Rajendra Prasad[c]

Abstract: The optimized investigations of gold nanoparticles (GNP) doped cholesteric liquid crystals revealed the vibrant transitions of liquid crystal phases. Thermodynamical investigation observed the critical temperatures of different phases. The different concentration of gold nanoparticles induced in cholesteric liquid crystal shows the extensive assortment of various phases and reduced the cholesteric-blue phase-isotropic transition temperature from 105 °C to 101 °C. The predisposition of the twisting of molecules in the gold nanoparticles doped cholesteric liquid crystal samples was confirmed by the electro-optical examination. Dielectric investigation recorded the effect of gold nanoparticles in cholesteric liquid crystal. It signatures that the dielectric permittivity and absorption reduced from 11.57 to 10.2 and 14 to 13.2 respectively. Plasmonic behavior of the CLC-Au NPs matrix modulated by the wavelength shifting. Enrichment of the functional area of the material surface and decrement of photoluminescence intensity has been experiential by the doping of gold nanoparticles in a cholesteric liquid crystals matrix.

Keywords: Photoluminescence; Plasmonic behavior; Dielectric investigation; Gold nanoparticles (Au-NPs).

INTRODUCTION

Liquid crystal is a unique and transitional phase between the solid and liquid. According to the arrangement of molecules liquid crystals have various phases (Qi & Hegmann, 2008; Coles & Morris, 2010; Infusino, *et al.*, 2013). The dispersion and unification of gold nanoparticles (GNP) into liquid crystals introduced very great progressive applications (Bisoyi & Kumar, 2011; Jain *et al.*, 2006; Daniel & Astruc, 2004). GNPs are one of the most famous and frequently studied metal which produces massive impact on various properties like optical, mechanical chemical, biological sensing, cancer treatment and electronic applications (Pathinti *et al.*, 2021; Asiya *et al.*, 2020; Lee *et al.*, 2016; Vardanyan *et al.*, 2013). This is theoretical and experimentally proved that, the liquid crystal materials have the self assembled nature of molecules by applying the external treatment. The bottom-up technique of plasmonic GNPs nanoparticles is realized by the liquid crystal because of their unique properties (Garbovskiy, 2017; Bitar *et al.*, 2011). GNPs nano particles are arranged in long order for the examination of physical properties of molecular order in the range of microscopic to the macroscopic level. The combined exhilaration of free electron charge carriers, which are present in the conduction band,

[a] Department of Physics, JSS Academy of Technical Education, Noida, India.
Corresponding author: dr_manisha@jssaten.ac.in

[b] Department of Biological Science, S. A. P. Kanya Mahavidyalaya, Kichha, India.

[c] Department of Applied Science, Galgotia's College of Engineering & Technology, Greater Noida, India.

of the GNP shows surface plasmon resonance (Tomylko *et al.*, 2011; Cordoyiannis *et al.*, 2020; Ding*et al.*, 2013). Surface plasmon resonance is a very important property for nano-optical devices (Chaudhary & Ghildyal, 2024; Yadav *et al.*, 2018; Roy *et al.*, 2019; Hadjichristov & Marinov, 2017; Pathak *et al.*, 2021). The optical and electrical performance such as brightness and efficiency are influenced by luminescence and dielectric investigation which are responsible for the doping of GNPs. The chirality of constitutional molecules forms the spiral structure of the cholesteric liquid crystal. Electric fields play a major role in optical devices. Due to the applied electric field to the liquid crystal materials then all molecules are aligned according to the direction of the electric field. That's why, selective light reflection property is very important for most optical active applications.

The focus of the present work is to examine the outcome of doping of GNPs (Au-NPs) in a thermotropic cholesteric liquid crystal (CLC). We presented here experimental results on pure and gold nanoparticles doped cholesteric liquid crystal. Thermal properties e.g. transition temperature and enthalpies of different mesophases of pure and GNPs doped cholesteric liquid crystal have been investigated. The molecular director shows the average direction of molecules in cholesteric liquid crystal. It has a helical structure. The helical pitch is the equivalent wavelength of visible light. The helical pitch of cholesteric liquid crystal lies in the visible light range of wavelength of visible light. Dispersion of GNPs modifies the helical pitch of cholesteric liquid crystal (Kim *et al.*, 2015). We have also investigated the dielectric properties, photoluminescence and plasmonic behavior of both pure and Au NPs dispersed cholesteryl butyrate cholesteric liquid crystal.

METHOD AND MATERIALS

In the extant study, the pure and Au NPs doped cholesteryl butyrate cholesteric liquid crystal (CB-CLC) have been used. The molecular formula and molecular weight of cholesteryl butyrate are $C_{21}H_{25}N$ and 291.44 respectively. Cholesteryl Butyrate (CB) Cholesteric liquid crystal has the following phase sequences, (a) crystalline phase (Cr), (b) cholesteric phase (N*), (c) blue phase (BP) and (d) isotropic phase (Iso). The cholesteryl butyrate cholesteric liquid-crystal (CB - CLC) and gold nanoparticles (Au NPs) have been procured by Sigma Aldrich. Without any fine-tuning of Cholesteric liquid crystal (CB) and gold nanoparticles (Au NPS), both have been used for various investigations. In the existing study, Cholesteric Liquid Crystal cholesteric butyrate (CB-CLC) and Au NPs were used as a host and dopant material respectively. The 10 nm was the particle size of the Au nanoparticles. We have organized four samples. Sample 1 referred to pure cholesteryl butyrate (CB) and 3 samples referred to the Au NPs (by different weight) dispersed cholesteryl butyrate. The host cholesteric liquid crystal is solid at room temperature. First, the Au NPs mixed with the ethanol solution. After that Au NPs become stabilised by the covering. In the second step, we dispersed the Au NPs in the host CB cholesteric liquid crystal as a dopant. After that, Au NPs doped cholesteric samples have been intermingling unceasingly and stimulated at a temperature of 100 °C. The ethanol solvent has been completely evaporated. Accordingly, we have prepared three Au NPs doped samples by weight of 0.5%, 1.0% and 1.5% in the cholesteryl butyrate cholesteric liquid-crystal (CB-CLC).

For the investigation of various properties of undoped cholesteryl butyrate cholesteric liquid crystal and Au NPs doped CLC, we have used conducting glass plates, and Indium tin oxide (ITO), for the preparation of liquid crystal cells prepared liquid crystal cells. The thickness of the cell was 6 μm. The isotropic phase of pure and Au NPs doped CB liquid crystal samples have been filled in the conducting liquid crystal cells by the capillary process. Differential scanning calorimeter (DSC) has been used for the thermodynamical examination of various liquid crystal phases of Au NPs dispersed and pure cholesteric butyrate liquid crystal. Photo Luminescence spectra of undoped binary mixture and GNPs doped binary mixture of liquid crystal have been recorded by using a Fluorescence Spectro photo-meter. Fluorescence Spectro photo-meter associated with a Xenon flash lamp in the mode of fluorescence. Agilent Carry Eclipse G9800A is the model's name for the fluorescence spectro photo-meter. The dielectric investigation of pure and Au NPs doped of cholesteryl butyrate cholesteric liquid-crystal has been measured by using an impedance analyzer. The model no of the impedance analyzer is HP 4192A. All the dielectric observations were computer-controlled and automated.

RESULT AND DISCUSSION

Thermodynamical studies

The differential scanning calorimetric apparatus achieved excellent thermal stability and operated at a slow scanning rate. DSC thermograms of undoped and Au NPs doped cholesteryl butyrate cholesteric liquid crystal are shown in Fig. 1. DSC thermogram has been recorded during the heating cycle at the 5 °C/min scanning rate. The 5.0 mg was the mass of all samples. The DSC thermograms reveal, heat capacity with the function of temperature of undoped CB cholesteric liquid crystal, 0.5 %, 1.0 % and 1.5 % by weight Au NPs doped CB cholesteric liquid crystal are exposed in figure 1 (a-d) respectively. DSC thermogram of undoped CB cholesteric liquid crystal (fig. 1a) has three peaks. The first peak agrees with the crystal (Cr) to cholesteric phase (N*) transition at 93 °C temperature, the transition of cholesteric phase (N*) to blue phase (BP) correlates with the second peak at 100 °C temperature and the third peak correspond with the transition of blue phase (BP) to isotropic phase (Iso) at 105 °C temperature.

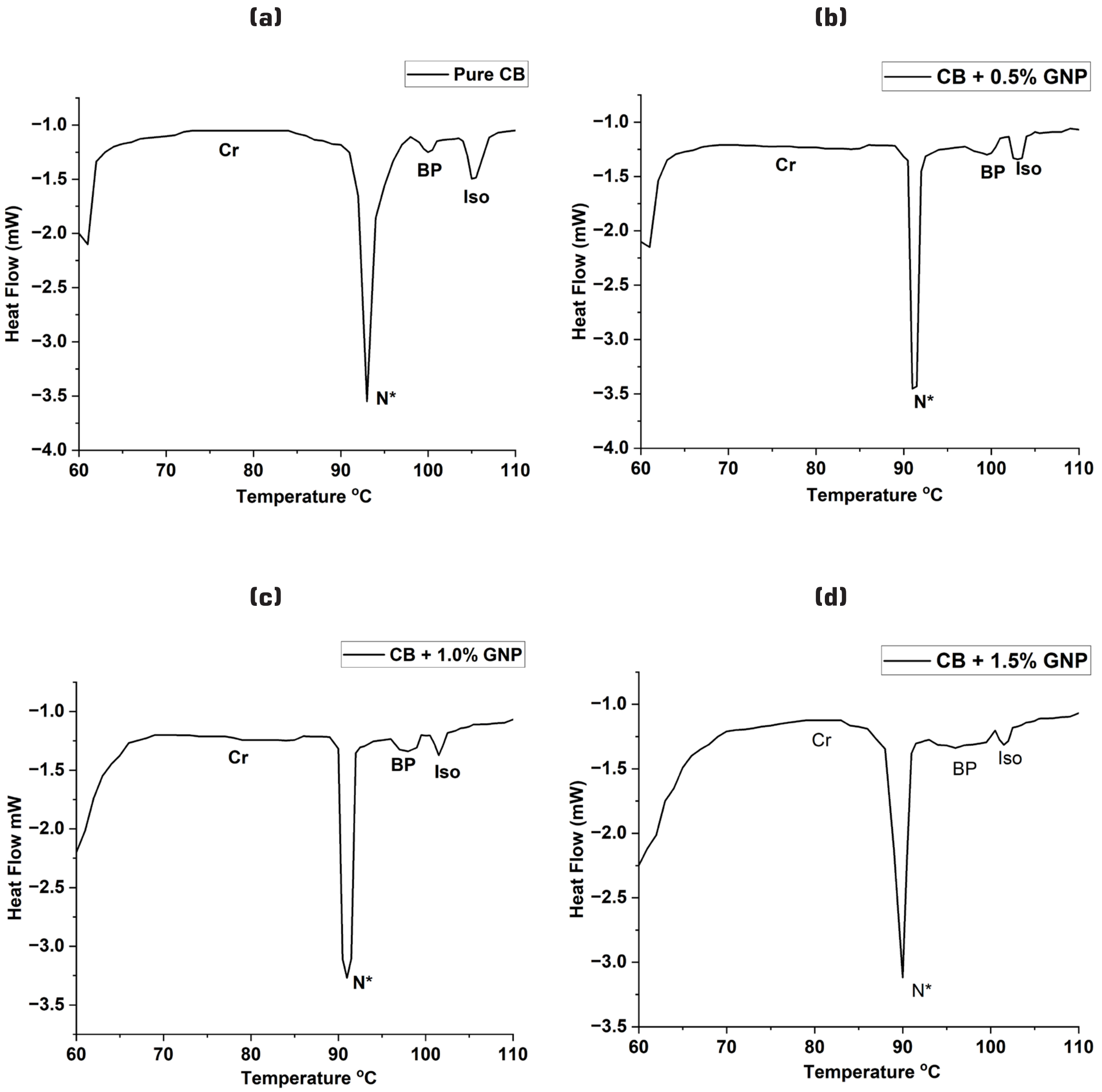

Figure 1. DSC thermograms of pure (a) and 0.5%, 1.0%, and 1.5% (b. c & d) gold nanoparticle doped CB cholesteric liquid crystal.

The DSC thermogram of Au NPs (0.5%, 1.0% and 1.5% by weight) doped CB cholesteric liquid crystal are shown in fig.1(b-d). The transition temperatures of crystalline phase (Cr) to cholesteric phase (N*), cholesteric phase (N*) to blue phase (BP) and blue phase (BP) to isotropic (Iso) phase of Au NPs doped sample 2 (0.5 % Au NPs doped CB) are 91.5 °C, 99.5 °C and 103 °C respectively. Similarly, Au NPs doped sample 3 (1.0 % Au NPs doped CB) has three peaks. The crystalline phase (Cr) to cholesteric phase (N*) transition corresponds to the first peak at 91 °C temperature, the second peak shows the transformation of the cholesteric phase (N*) to blue phase (BP) at 98 °C temperature and the third peak correspond with the conversion of blue phase (BP) to isotropic phase (Iso) at 101.5 °C temperature. The transition temperatures of crystalline phase (Cr) to cholesteric phase (N*), cholesteric phase (N*) to blue phase (BP) and blue phase (BP) to isotropic phase (Iso) of Au NPs doped sample 4 (1.5 % Au NPs doped CB) are 90 °C, 96 °C and 101 °C respectively.

In the present study, the dispersion of Au NPs in the CB Cholesteric liquid crystal reduced gradually conversion temperatures and enthalpies of crystalline (Cr) to cholesteric (N*), cholesteric (N*) to blue phase (BP) and blue phase (BP) to isotropic (Iso) transition with the cumulative of doping percentage of Au NPs in the unadulterated CB cholesteric liquid crystal. Another interesting feature of Au NPs doped CB CLC samples is the range of the blue phase increased with the increasing doping of Au NPs (Fig. 1b-d). The doping of Au NPs does imply the very specific determination of transition temperature and increment of range of blue phase. The first order of transition of the blue phase depends on the latent heat and it plays a major role (Bukowczan *et al.*, 2021). The blue phase sturdily stabilized in the occurrence of Au NPs. The changing of enthalpies is dependent on the conversion of various phases (Cr, N*, BP and Iso) in undoped and Au NPs doped CB cholesteric liquid crystal. We are also experiential that the distinction of the transition temperature of different phases of pure CB cholesteric liquid crystal is greater as associated with Au NPs doped CB cholesteric liquid crystal. The encouragement of doping on the conversion temperature resembles the mean-field theory hypothetical model of cholesteric liquid crystal (Gorkunov & Osipov, 2011; Petriashvili, 2022).

Photoluminescent Study

In the present study, photoluminescent (PL) spectra of undoped and Au NPs doped CB-CLC samples were recorded at room temperature and shown in Fig. 2. The excitation wavelength was 410 nm for the investigation of luminescence properties in the

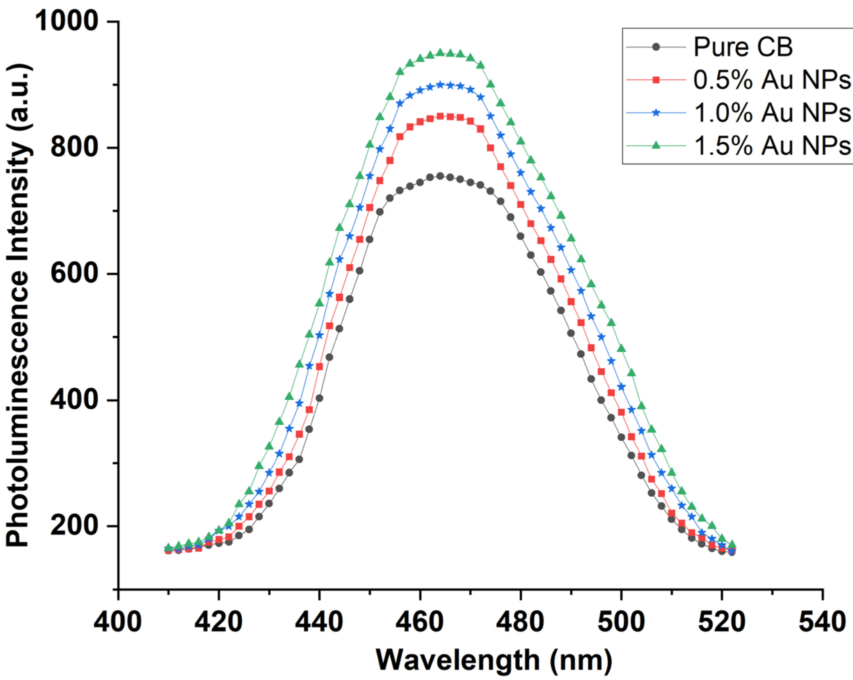

Figure 2. Photoluminescence Spectra of pure and Au-NPs doped CB cholesteric liquid crystal.

 https://doi.org/10.37819/nanofab.009.2029

influence of increasing doping of Au NPs in CB cholesteric liquid crystal as well as in undoped CB cholesteric liquid crystal. The photoluminescence intensity of undoped and Au NPs doped CB cholesteric liquid crystal was maximum at 464 nm wavelength. The photoluminescence intensity of undoped cholesteric liquid crystal CB was 755 a.u. Further, the addition of (0.5%, 1.0% & 1.5% by weight) Au NPs in the CB cholesteric liquid crystal exhibited the photoluminescence intensity 850, 900, 950 a.u. respectively. Fig. 2 shows that the luminescence intensity continuously increased due to the increment of doping of Au NPs. The size of Au NPs played a significant role in the enhancement of PL intensity. This enhancement is attributed to the accumulation and surface functionality of Au NPs (Huang, 2015; Kumar & Singh, 2023). The photoluminescence properties of the display depend on the suitable dopant's particle size. It increases the addingexcitation reflections and PL intensity becomes enhanced (Chaudhry & Ghildyal, 2022).

Plasmonic Investigation

The plasmonic behavior of undoped CB-CLC and doped CB-CLC are shown in Fig.3. Fig. 3 presents the absorption spectra of undoped CB-CLC. The absorption peak of undoped CB-CLC was observed around 570 nm and shows the absorption spectra of Au NPs doped CB-CLC samples. 0.5% Au NPS doped CB-CLC has an absorption peak of 535 nm, 1.0% Au NPS doped CB-CLC has an absorption peak of 534 nm and 1.5% Au NPS doped CB-CLC has an absorption peak of 533 nm. The reflection central wavelength λ_o shifts from 570 nm to 535 nm due to the doping of Au NPs in the cholesteryl butyrate cholesteric liquid crystal. The shifting of the reflection central wavelength λ_o is due to the orientation of the helix axis (Roy *et al.*, 2015). Due to the scattering of light by the boundaries of liquid crystal cells, it introduced the loss of transmission of light. That's why the reflection central wavelength λ_o shifted towards the lower wavelengths. This lag of shifting of reflection central wavelength λ_o is responsible for analytically reproducible (De *et al.*, 2018).

Fig. 3 shows the plasmonic properties of the undoped and Au NPs particles doped CB cholesteric liquid crystal. Basically, an increment of absorbance accredited the plasmonic behavior of Au NPs. It is a well-known fact that the circularly polarised light is reflected by the layers of cholesteric liquid crystal. This is notable by the surface plasmon resonance (SPR). The reflection of circularly polarised light by the undoped CB Cholesteric liquid crystal at 550 nm.

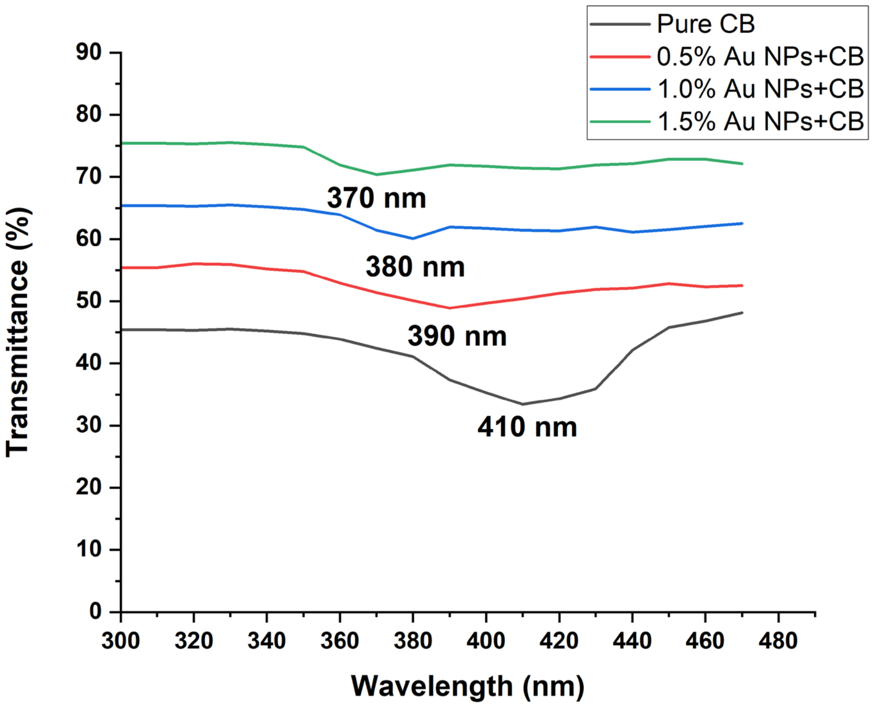

Figure 3. Plasmonic Spectra of pure and Au-NPs doped CB cholesteric liquid crystal.

Dielectric Study

In the present work, the dielectric characteristics of the undoped and Au NPs doped CB cholesteric liquid crystal samples were investigated by dielectric spectroscopy technique (Caputo *et al.*, 2012; Liu *et al.*, 2018). This is a very influential technique for the consideration of molecular particulars. The dielectric properties have been recorded as a function of the frequency of undoped and Au NPs dispersed CB cholesteric liquid crystal samples. Fig. 4 Shows the dielectric permittivity.

The most significant physical property of the liquid crystal is dielectric anisotropy. The operating verge voltages for liquid crystal displays are evaluated by the dielectric anisotropic. The multifaceted dielectric constant of the liquid crystal is expressed with the equation (Chauhan, 2023).

$$\varepsilon* = \varepsilon' - i\varepsilon'' \quad (1)$$

The dielectric constant has real (ε') and imaginary parts (ε'') respectively. The imaginary part ε" illustrates the dielectric loss. Fig. 4a demonstrates the frequency-dependent dielectric permittivity ε' of undoped and Au-NPs doped CB-CLC at room temperature. The dielectric permittivity of undoped and Au NPs doped CB-CLC is continuously decreased with increasing frequency. In Fig 4a, it is clear that the dielectric permittivity decreases due to the increment of doping of Au NPs in CLC. The dielectric permittivity which has a high value at 1K. A potential barrier is generated at low frequency due to the existence of space charge polarization. The maximum variation of dielectric permittivity is achieved in the range of frequency 1K to 100K due to the attenuation of space charge polarization. After that, the variation of dielectric permittivity remains constant from 10K to 100K. Due to the lack of sufficient time at high frequencies, the molecules do not align in the direction of the applied electric field. Dielectric absorption spectra of undoped and doped are shown in the Fig 4b. Initially the dielectric loss factor ε" increases with the increasing of frequency. It reaches up to the maximum value at a critical value of frequency and then decreases with further frequency increases. The dielectric absorption of undoped and doped CB - CLC attain a maximum peak at 520992 Hz frequency. The dielectric absorption decreases with the increasing doping of Au NPs by weight. The information of movement and bonding of molecules is satisfied by the transition frequency (Köysal, 2010; Jonscher, 1999; Infusino *et al.*, 2014).

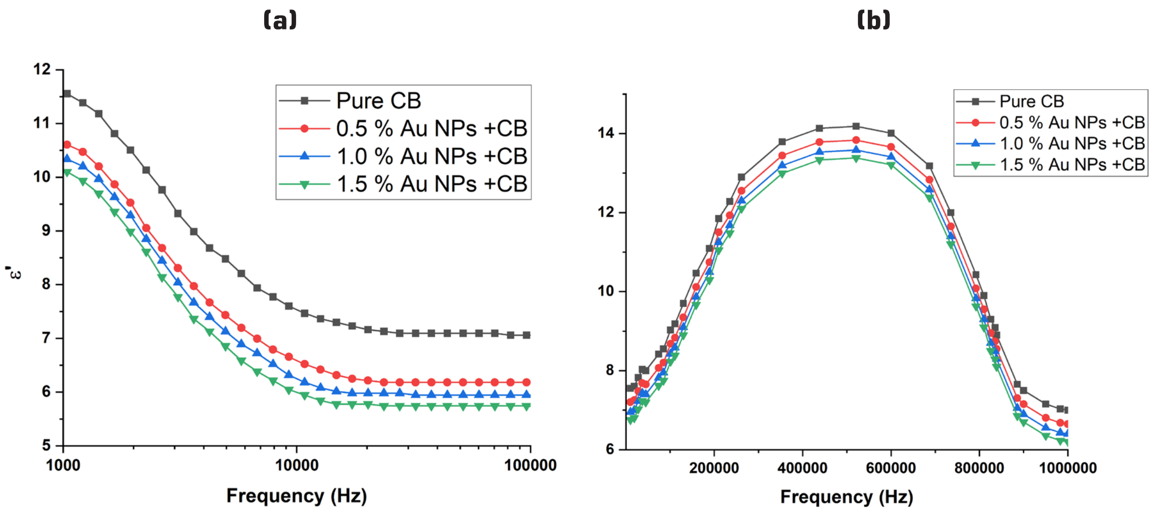

Figure 4. Dielectric investigation (a) permittivity and (b) absorption spectra of pure and Au-NPs doped CB cholesteric liquid crystal.

CONCLUSION

We dispersed Au NPs in a Cholesteryl butyrate cholesteric liquid crystal and investigated the outcome of Au-NPs on thermodynamical, photoluminescence, plasmonic and dielectric properties. Thermodynamical studies stated that the dispersion of Au NPs in cholesteryl butyrate directed towards a lessening of the critical temperatures of cholesteric (N*) and blue phase. The critical temperatures of cholesteric

 https://doi.org/10.37819/nanofab.009.2029

(N*) and blue phase (BP) were reduced due to the dispersion of Au-NPs. An anisotropic nature is very weak in the Au nanoparticles. That's why the decrement of critical temperature is a connotation with the anisotropic properties' effect of Au nanoparticles. The percentage of doping and size of Au NPs play a very important for reducing the temperature. Photoluminescence spectra show the Au-NPs heightened photoluminescence properties of cholesteryl butyrate. The signature of the high functionality of Au-NPs explicitly the interaction between the surface of the host and doped material. The electromagnetic field is generated at the surface of Au NPs due to the interaction between the molecules. The Au-NPs and cholesteryl butyrate matrix change so many optical properties. This matrix has excessive latent for the photonics devices. Au-NPs contribute a major role in the enhancement of plasmonic properties of cholesteryl butyrate cholesteric liquid crystal. We observed a significant change in the transmission behavior. The transmission responses are shifted towards the lower wavelength due to the increasing refractive index. The wavelength shifting is responsible for the shape and molecular arrangement of Au NPs doped CB-CLC matrix. Impedance analysis showed the existence of Au NPs due to the charge accumulation at the edge. Dielectric studies signified that the decrement of dielectric permittivity and absorption of CB cholesteric liquid crystal due to doping of Au NPs suggested the orientation of molecules is reduced. The dipole correlation of CLC molecules also changed due to the Au NPs matrix. So ionization, recombination of molecules and ionic conductivity of CLC-Au NPs matrix has been increased. The CLC-Au NPs matrix is a very important candidate for liquid crystal displays in the future. This composite will tune the various properties of optical devices.

Conflict of Interest

The authors declare that they don't have any known rival financial interests or personal relationships that could have been shown to influence the work reported in this paper.

Acknowledgments

This research work is supported by the National Physical Lab (CSIR) and Thapar Institute of Engineering and Technology, Patiala, for providing necessary experimental facilities. ♦

REFERENCES

Asiya, S., Pal, K., Kralj, S., & Thomas, S. (2020). Nanomaterials dispersed liquid crystalline self-assembly of hybrid matrix application towards thermal sensor. Nanofabrication for Smart Nanosensor Applications, chapter-12, 295-321. https://doi.org/10.1016/B978-0-12-820702-4.00013-1

Bisoyi, H. K., & Kumar, S. (2011). Liquid-crystal nanoscience: an emerging avenue of soft self-assembly. Chemical Society Reviews, 40, 306-319. https://doi.org/10.1039/B901793N

Bitar, R., Agez, G., & Mitov, M. (2011). Cholesteric liquid crystal self - organization of gold nanoparticles. Soft Matter, 7, 8198-8206. https://doi.org/10.1039/C1SM05628J

Bukowczan, A., Hebda, E., & Pielichowski, K. (2021). The influence of nanoparticles on phase formation and stability of liquid crystals and liquid crystalline polymers. Journal of Molecular Liquids, 321, 114849. https://doi.org/10.1016/j.molliq.2020.114849

Caputo, R., De, S. L., Cataldi, U., & Umeton, C. (2012). Plasmon Resonance Tunability of Gold Nanoparticles Embedded in a Confined Cholesteric Liquid Crystal Host. Molecular Crystal Liquid Crystal, 559, 194-201. https://doi.org/10.1080/15421406.2012.658709

Chaudhary, M., & Ghildyal, D. (2024). Investigations of axioms of twist grain boundary phases (TGBPs) in binary mixture of liquid crystals. International Journal of Modern Physics B, 38, 2450006 https://doi.org/10.1142/S0217979224500061

Chaudhry, M., & Ghildyal, D. (2022). Characterization of thermal, electro optical and photoluminescent properties of nematic liquid crystal doped with gold nano particles. Materials today: Proceedings, 57, 2061-2066. https://doi.org/10.1016/j.matpr.2021.11.265

Chauhan, G., Malik, P., & Deep, A. (2023). Morphological, dielectric, electro-optic and photoluminescence properties of titanium oxide nanoparticles enriched polymer stabilized cholesteric liquid crystal composites. Journal of Molecular Liquids, 376, 121406. https://doi.org/10.1016/j.molliq.2023.121406

Coles, H., & Morris, S. (2010). Liquid Crystal lasers. Nature Photonics, 4, 676-685. http://doi.org/10.1038/nphoton.2010.184

Cordoyiannis, G., Lavric, M., Treck, M., Tzitzios, V., Lelidis, I., Nounesis G., Daniel, H., & Kutnjak, Z. (2020). Quantum Dot-Driven Stabilization of Liquid-Crystalline Blue Phases. Frontiers in Physics, 8, 1-8. https://doi.org/10.3389/fphy.2020.00315

Daniel, M. C., & Astruc, D. (2004). Gold nanoparticles: Assembly, supramolecular chemistry, quantum-size-related properties, and applications toward biology, catalysis, and nanotechnology. Chemical Reviews, 104, 293-346. https://doi.org/10.1021/cr030698+

De, S. L., Cataldi, U., Guglielmelli, A., Bürgi, T., Tabiryan, N., Bunning, T. J. (2018). Dynamic optical properties of gold nanoparticles/cholesteric liquid crystal arrays. MRS Communications, 8, 550-555. https://doi.org/10.1557/mrc.2018.80

Ding, H., Wang, X., Mu, L., Yang, Z., Yang, H. (2013). The Effect of CB15 on Cholesteric Liquid Crystal's Thermal-Optical Properties. Advanced Materials Research, 807, 2684-2687. https://doi.org/10.4028/www.scientific.net/AMR.807-809.2684

Garbovskiy, Y. (2017). Ions in liquid crystals doped with nanoparticles: conventional and counterintuitive temperature effects. Liquid Crystal, 44, 1402-1408. https://doi.org/10.1080/02678292.2017.1280856

Gorkunov, M. V., & Osipov, M. A. (2011). Mean-field theory of a nematic liquid crystal doped with anisotropic nanoparticles. Soft Matter, 7, 4348-4356. https://doi.org/10.1039/C0SM01398F

Hadjichristov, G. B., & Marinov, Y. G. (2017). Photo responsive azo-doped aerosil/7CB nematic liquid-crystalline nanocomposite films: the role of polyimide alignment layers of the films. Journal of Physics: Conference Series, 780, 012008. https://doi.org/10.1088/1742-6596/780/1/012008

Huang, C. C., Chou, T. R., Chen, J. W., & Chao, C. Y. (2015). Enhancement of Photoluminescence Intensity of Cd Se Nanorods doped in cholesteric liquid crystals. Brazilian Journal of Physics, 45, 41-46. https://doi.org/10.1007/s13538-014-0284-9

Infusino, M., De, L. A., Ciuchi, F., Ionescu, A., Scaramuzza, N., & Strangi, G. (2014). Optical and electrical characterization of a gold nanoparticle dispersion in a chiral liquid crystal matrix. Journal of Materials Science, 49, 1805-1811. https://doi.org/10.1007/s10853-013-7868-6

Infusino, M., Luca, A. D., Ciuchi, F., Ionescu, A., Scaramuzza, N., & Strangi, G. (2013). Effects of Gold Nanoparticle Dispersion in a Chiral Liquid Crystal Matrix. Molecular Crystal Liquid Crystal, 572, 59-65. https://doi.org/10.1080/15421406.2012.763211.

Jain, P. K., Lee, K. S., El-Sayed, I. H., & El-Sayed, M. A. (2006). Calculated absorption and scattering properties of gold nanoparticles of different size, shape, and composition: applications in biological imaging and biomedicine. The Journal Physical Chemistry B, 110, 7238-7248. https://doi.org/10.1021/jp057170o

Jonscher, A. K. (1999). Dielectric relaxation in solids. Journal of Physics D: Applied Physics, 32, R57-R70. https://doi.org/10.1088/0022-3727/32/14/201

Kim, H., Kobashi, J., Maeda, Y., Yoshida, H., & Ozaki, M. (2015). Pitch-Length Independent Threshold Voltage of Polymer/Cholesteric Liquid Crystal Nano-Composites. Crystals, 5, 302-311. https://doi.org/10.3390/cryst5030302

Köysal, O. (2010). Conductivity and dielectric properties of cholesteric liquid crystal doped with single wall carbon nanotube. Synthetic Metals, 160, 1097-1100. https://doi.org/10.1016/j.synthmet.2010.02.033

Kumar, A., & Singh, G. (2023). Recent advances and future perspectives of photoluminescent liquid crystals and their nanocomposites for emissive displays and other tunable photonic devices. Journal of Molecular Liquids, 386, 122607. https://doi.org/10.1016/j.molliq.2023.122607

Lee, H. G., Munir, S., & Park, S. Y. (2016). Cholesteric liquid crystal droplets for biosensors. ACS Applied Materials Interfaces, 8, 26407-26417 https://doi.org/10.1021/acsami.6b09624

Liu, Y. S., Lin, H. C., & Xu, H. L. (2018). The Surface Plasmon Resonance Effect on the Defect-Mode Cholesteric Liquid Crystals Doped with Gold Nanoparticles. IEEE Photonics Journal, 10, 4700407. https://doi.org/10.1109/JPHOT.2018.2821560

Pathak, G., Hegde, G., & Prasad, V. (2021). Octadecylamine-capped CdSe/ZnS quantum dot dispersed cholesteric liquid crystal for potential display application: Investigation on photoluminescence and UV absorbance. Liquid Crystal, 48, 579-587. https://doi.org/10.1080/02678292.2020.1799085

Pathinti, R S., Gollapelli, B., Jakka, S. K., & Vallamkondu, J. (2021). Green synthesized TiO_2 nanoparticles dispersed cholesteric liquid crystal systems for enhanced optical and dielectric properties. Journal of Molecular Liquids, 336, 116877-84. https://doi.org/10.1016/j.molliq.2021.116877

Petriashvili, G., Devadze, L., Zurabishvili, T., Sepashvili, N., Chirakadze, A., Bukia, T., &

Sanikidze, G. (2022). Gold nanoparticles mediated tuning of thermo-optical parameters in gold nanoparticles doped cholesteric liquid crystal nanocomposite. Nano Studies, 22, 111-124. https://doi.org/10.52340/ns.2022.12

Qi, H., & Hegmann, T. (2008). Impact of nanoscale particles and carbon nanotubes on current and future generations of liquid crystal displays. Journal of Materials Chemistry. 18, 3288-3294. https://doi.org/10.1039/B718920F

Roy, J. S., Majumder, T. P., & Dabrowski, R. (2015). Photoluminescence behavior of TiO2 nanoparticles doped with liquid crystals. Journal of Molecular Structure, 1098, 351-354. https://doi.org/10.1016/j.molstruc.2015.06.028

Roy, A., Singh, B. P., Yadav, G., Khan, H., Kumar, S., Srivastava, A., & Manohar, R. (2019). Effect of gold nanoparticles on intrinsic material parameters and luminescent characteristics of nematic liquid crystals. Journal of Molecular Liquid, 295, 111872. https://doi.org/10.1016/j.molliq.2019.111872

Tomylko, S., Yaroshchuk, O., Kovalchuk, O., Maschke, U., & Yamaguchi, R. (2011). Dielectric and electro-optical properties of liquid crystals doped with diamond nanoparticles. Molecular Crystal Liquid Crystal, 541, 273-281. https://doi.org/10.1080/15421406.2011.569658

Vardanyan, K. K., Sita, D. M., Walton, R. D., Saidel, W. M., & Jones, K. M. (2013). Cyanobiphenyl liquid crystal composites with gold nanoparticles. RSC Advances, 3, 259−273. https://doi.org/10.1039/C2RA21220J

Yadav, G., Katiyar, R., Pathak, G., & Manohar, R. (2018.) Effect of ion trapping behavior of TiO2 nanoparticles on different parameters of weakly polar nematic liquid crystal. Journal of Theoretical and Applied Physics, 12, 191-198. https://doi.org/10.1007/s40094-018-0296-x